Communication

Size-Controlled Synthesis of Magnetic CuCrSe Nanocrystals

Yu-Hsiang A. Wang, Ningzhong Bao, Liming Shen, Prahallad Padhan, and Arunava Gupta

J. Am. Chem. Soc., **2007**, 129 (41), 12408-12409• DOI: 10.1021/ja075893a • Publication Date (Web): 26 September 2007

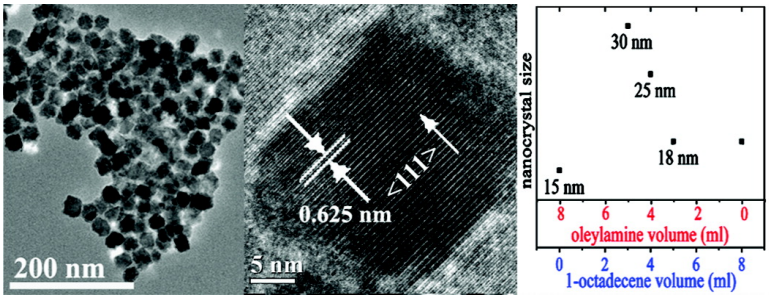

More About This Article

Additional resources and features associated with this article are available within the HTML version:

- Supporting Information
- Links to the 2 articles that cite this article, as of the time of this article download
- Access to high resolution figures
- Links to articles and content related to this article
- Copyright permission to reproduce figures and/or text from this article

View the Full Text HTML

J|A|C|S
COMMUNICATIONS

Published on Web 09/26/2007

Size-Controlled Synthesis of Magnetic $CuCr_2Se_4$ Nanocrystals

Yu-Hsiang A. Wang, Ningzhong Bao, Liming Shen, Prahallad Padhan, and Arunava Gupta*

Department of Chemistry and Center for Material for Information Technology, University of Alabama, Tuscaloosa, Alabama 35487

Received August 6, 2007; E-mail: agupta@mint.ua.edu

The controlled synthesis of inorganic nanocrystals (NCs) has generated much interest in recent years, motivated in large part by the unusual electronic, optical, and magnetic properties that are exhibited in this size regime.[1] Controlling the growth of NCs of widely divergent shapes and sizes is nontrivial, and in most cases the crystals adopt thermodynamically favored forms, including spheres, cubes, hexagons, rods, wires, etc.[2] The solution-based synthesis of a wide range of magnetic NCs of different morphologies has been reported, including those of transition metals (Fe, Co, Ni), alloys (FePt, CoPt, etc), and oxide materials (ferrites, perovskites, etc).[1,3] Their properties have been studied quite extensively, both from the viewpoint of fundamental understanding and applications, ranging from magnetic resonance imaging, drug delivery, biosensing, and nanoelectronic devices.[3] These studies notwithstanding, the synthesis and properties of a number of other nanocrystalline magnetic materials, such as those based on the rare earths and chalcogenides, remain largely unexplored. Of particular interest are the chromium-based spinel chalcogenides, ACr_2X_4 (A = Cu, Cd, Hg, Fe, Co; X = S, Se, Te),[4] which are ferro/ferrimagnetic insulators, semiconductors, or even metals that display unique properties in the bulk.[5,6] As in the case of the standard magnetic systems, the utility of the chalcospinels can be augmented if they can be synthesized as colloidal nanocrystals with highly controlled dimensions.

Room-temperature ferromagnetism with a Curie temperature of 430 K makes $CuCr_2Se_4$ an interesting system of study among the chalcospinels.[4] Additionally, it is metallic and exhibits a pronounced magneto-optic Kerr effect at room temperature.[6] Solution-based synthesis of $CuCr_2Se_4$ and other chalcospinels has, however, been limited by the complexity involved in the synthesis, particularly since they cannot be precipitated from aqueous solution. Furthermore, it is difficult to synthesize the stoichiometric compound and/or the desired spinel phase because of the volatility of Se and the availability of a number of oxidation states of chromium.[4,7] Recently, there have been reports of solution-based solvothermal[8] and microwave synthesis[9] of $CuCr_2Se_4$ crystals. While the phase-pure material has been stabilized, these reactions result in the formation of relatively large crystallites or agglomerates with a broad size and shape distribution. Herein we report on the facile synthesis of size-controlled $CuCr_2Se_4$ nanocrystals (~15−30 nm) that are nearly monodisperse and readily form a colloidal suspension. The process involves the thermal decomposition and reaction of the metal−acetylacetonate precursors with selenium in a high-boiling organic solvent mixture of oleylamine (OLA) and 1-octadecene (ODE). The coordinating solvents play the dual role of forming an organo−Se intermediate and in selectively adsorbing on the surface of the nucleated product to passivate and control their size. This obviates the need of using a separate reducing agent (such as β-sitosterol[8]) and surfactant for the reaction process.

All the reactions were performed in a fume hood, under inert conditions, and elemental Se was disposed of using safe laboratory techniques. In a typical reaction for the synthesis of 15-nm average diameter NCs, 2.4 mmol selenium (Se) powder was dissolved in 8 mL of OLA at 330 °C under nitrogen atmosphere and then cooled down to room temperature. Separately, 0.3 mmol of copper (II) acetylacetonate (acac) and 0.6 mmol of chromium (III) acetylacetonate (acac) were co-dissolved in 2 mL of OLA at ~175 °C under vacuum and then backfilled with nitrogen. After cooling down to room temperature, the mixture was injected under nitrogen atmosphere into the Se solution and the resulting mix heated up to 350 °C in 30 min. The reaction mixture was maintained at this temperature for 1 h while being continually stirred, during which a brown-black solution was formed. After the mixture cooled down to room temperature, a mixture of hexane and ethanol (1:3) was added to the solution, and a black product with yield in the range of 70−85% was precipitated via centrifugation (6000 rpm). The average size of the NCs could be systematically increased up to 30 nm by using a solvent mixture of OLA and ODE. For example, to synthesize 25-nm $CuCr_2Se_4$ NCs, a solvent mixture ODE and OLA with volume ratio of 1:1 was used for dissolution and formation of the selenium compound. The other reaction steps were the same as those used for the synthesis of the smaller NCs. Interestingly, for higher concentrations of ODE (above ~75%) the average size again decreased, with ~18-nm crystals being obtained using pure ODE (see SI).

We have found that Se with about 100% excess is optimum for the synthesis. A significantly broader size distribution of the product and/or formation of secondary phases, such as $CuCrSe_2$ (see SI), are observed at much higher or lower concentrations. Similarly, lowering the Se reaction temperature from 330 to 270 °C results in the formation of randomly shaped NCs. On the basis of nuclear magnetic resonance and mass spectral data we conclude that, while both ODE and OLA can react with Se at 330 °C, only the latter is effective at the lower temperature. The proposed mechanism for formation of the Se−ODE intermediate via allylic insertion is provided in the Supporting Information. On the basis of this and other reported mechanisms in the literature,[10,11] we propose the following reaction scheme using OLA as solvent: $Cu(acac)_2 + 2\ Cr(acac)_3 + 8\ C_{18}H_{36}NSeH \rightarrow Cu(C_{18}H_{36}NSe)_2 + 2\ Cr(C_{18}H_{36}NSe)_3 + 8\ (acac)\text{-}H \rightarrow CuCr_2Se_4 + C_{18}H_{35} + 4\ H_2Se + 8\ (acac)\text{-}H$. We have determined that tri-octyl phosphine is not suitable as a solvent because of its reaction with the chromium intermediate. Moreover, addition of oleic acid or tri-octyl phosphine oxide as surfactants to the OLA/ODE solvent mixture does not result in any significant size or shape variations.

The morphology of the synthesized nanocrystals has been investigated using TEM. As shown in Figure 1, the NCs synthesized using OLA+ODE, with an average size of 25 nm, exhibit close to cubic morphology. A similar shape is observed for the smaller sized NCs (see SI for TEM images of 18-nm crystals). The NCs are relatively monodisperse, as seen in Figure 1, with a size distribution of ±15%. A similar distribution is obtained for the 18-nm NCs. The inset to Figure 1 shows the high-resolution TEM (HRTEM) image of a NC that exhibits lattice fringes. A lattice spacing of *d*

10.1021/ja075893a CCC: $37.00

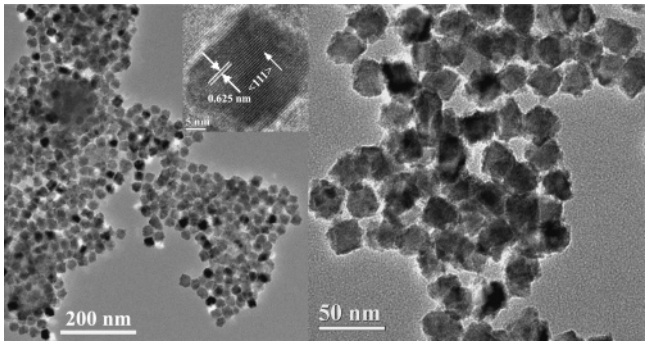

Figure 1. TEM and HRTEM images of $CuCr_2Se_4$ nanocrystals with an average size of 25 nm.

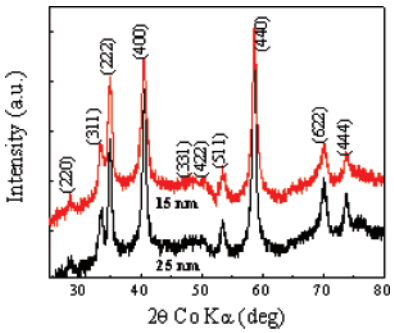

Figure 2. X-ray powder diffraction patterns (using a Co Kα source, λ = 1.789 Å) of (a) 15-nm and (b) 25-nm NCs.

= 0.625 nm is observed, corresponding to the (111) lattice planes of the face-central cubic chalcospinel phase.

As shown in Figure 2, the peak positions and relative intensities of all the X-ray diffraction peaks for the 15- and 25-nm NCs match well with the powder diffraction data for $CuCr_2Se_4$ (JCPDS No. 81-1986). As expected, the peaks are broader for the smaller sized NCs. From the peak widths, the average crystalline size is estimated to be 16.3 and 22.9 nm, respectively, which is in very good agreement with the TEM results. The composition has also been confirmed using energy dispersive X-ray analysis (EDX), which indicates that the Cu:Cr:Se concentration is very close to the expected 1:2:4 ratio for these two samples.

The magnetic properties of the nanocrystals have been measured using a superconducting quantum interference device (SQUID). Panels a and b in Figure 3 show the hysteresis loops for the NCs, with average size of 15 and 25 nm, measured at 300 and 10 K, respectively. Both the samples are superparamagnetic (SP) at room temperature but exhibit hysteretic behavior at 10 K with relatively low coercivity. The saturation magnetization (M_s) values at 10 K are 37 and 43 emu/gm for the 15- and 25-nm NCs, respectively. These are somewhat lower than the value of 56 emu/g reported in the bulk. Because of the small crystalline size, SP behavior at room temperature is not unexpected. The thermal energy can overcome the anisotropy energy barrier for these sizes, and the net magnetization of the NC assemblies in the absence of an external field averages to zero.[3,12] Based on Langevin fits[12] to the magnetization loops at 300 K (SI), the estimated sizes for the 15- and 25-nm NCs are 10.5 and 12.1 nm, respectively, qualitatively consistent with the actually observed average particle sizes. A larger deviation is observed for the latter, likely because of its being closer to the SP limit at 300 K. Figure 3c shows the temperature dependence of the field-cooled (FC) and zero-field-cooled (ZFC) magnetization results measured at different fields for the 25-nm NCs. While the Curie temperature is much above room temperature, the crystallites are ferromagnetic only below the blocking temperature of ~250 K as deduced from the low-field (50 Oe) measurements.

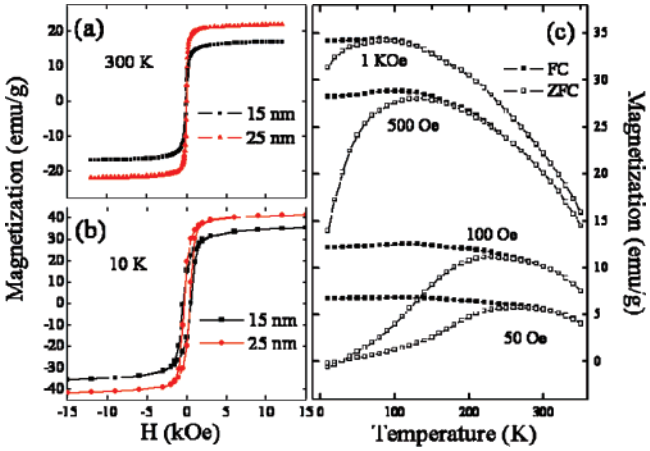

Figure 3. Magnetization as a function of field for the 15- and 25-nm NCs at (a) 300 K and (b) 10 K. (c) Magnetization versus temperature for field-cooled (FC) and zero-field-cooled (ZFC) measurements at different magnetic fields for the 25-nm NCs.

To summarize, we have developed a simple solution-based route for the synthesis of size-controlled cubic $CuCr_2Se_4$ nanocrystals. The process involves the thermal decomposition of the metal−acetylacetonate precursors and their reaction with Se complexed to high-boiling solvent mixtures of OLA and ODE. In addition to acting as surfactants, the coordinating solvents form organo−Se adducts via insertion. We believe that the process can be extended to the nanocrystal synthesis of a variety of other ternary chalcogenides, including chalcospinels and chalcopyrites (AB_2X_4 and ABX_2 [A = M^+ or M^{2+}, B = M^{3+}, X = S or Se]).

Acknowledgment. This work was supported in part by NSF Grant No. ECS-0621850. We are grateful to K. Belmore for NMR and Q. Liang for mass spectrometry measurements.

Supporting Information Available: The proposed scheme for the reaction of Se using ODE; nuclear magnetic resonance and mass spectral data; TEM of 18-nm NCs; XRD patterns of nanocrystals prepared using different percentages of excess Se; and the fitted Langevin functions for the magnetization data. This material is available free of charge via the Internet at http://pubs.acs.org.

References

(1) (a) Park, J.; Joo, J.; Kwon, S. G.; Jang, Y.; Hyeon, T. *Angew. Chem.* **2007**, *46*, 4630−4660. (b) Vanmaekelbergh, D.; Liljeroth, P. *Chem. Soc. Rev.* **2005**, *34*, 299−312. (c) Schmidt, G. *Nanoparticles: From Theory to Application*; Wiley-VCH: Wenheim, 2004. (d) Masala, O.; Seshadri, R. *Annu. Rev. Mater. Res.* **2004**, *34*, 41−81.
(2) Yin, Y.; Alivisatos, A. P. *Nature* **2005**, *437*, 664−670.
(3) Hyeon, T. *Chem. Commun.* **2003**, 927−934.
(4) (a) Nikiforov, K. G. *Prog. Cryst. Growth Charact. Mater.* **1999**, *39*, 1−104. (b) Goodenough, J.B.; Gräper, W.; Holtzberg, F.; Huber, D. L.; Lefever, R. A.; Longo, J. M.; McGuire, T. R.; Methfessel, S. *Magnetic and Other Properties of Oxides and Related Compounds*; Landolt-Börnstein: Numerical Data and Functional Relationships in Science and Technology; Group III: Crystal and Solid State Physics; Springer-Verlag: Weinheim, 1970; Vol. 4b.
(5) (a) Hemberger, J.; Lunkenheimer, P.; Fichtl, R.; von Nidda, H. A. K.; Tsurkan, V.; Loidl, A. *Nature* **2005**, *434*, 364−367. (b) Ramirez, A. P.; Cava, R. J.; Krajewski, J. *Nature* **1997**, *386*, 156.
(6) Brandle, H.; Schoenes, J.; Wachter, P.; Hullinger, F. *Appl. Phys. Lett.* **1990**, *56*, 2602−2603.
(7) Fedorov, V. A.; Kesler, Y. A.; Zhukov, E. G. *Inorg. Mater.* **2003**, *39*, S68−S88.
(8) Ramesha, K.; Seshadri, R. *Solid State Sci.* **2004**, *6*, 841−845.
(9) Kim, D.; Gedanken, A.; Tver'yanovich, Y. S.; Lee, D. W.; Kim, B. K. *Mater. Lett.* **2006**, *60*, 2807−2809.
(10) Steckel, J. S.; Yen, B. K. H.; Oertel, D. C.; Bawendi, M. G. *J. Am. Chem. Soc.* **2006**, *128*, 13032−13033.
(11) Choi, S.-H.; Kim, E.-G.; Hyeon, T. *J. Am. Chem. Soc.* **2006**, *128*, 2520−2521.
(12) Cullity, B. D. *Introduction to Magnetic Materials*; Addison-Wesley: Reading, MA, 1972.

JA075893A